Biotechnology Journal
www.biotechnology-journal.com

Sacrificial Bioprinting of a Mammary Ductal Carcinoma Model

*Margaux Duchamp, Tingting Liu, Anne M. van Genderen, Vanessa Kappings, Rahmi Oklu, Leif W. Ellisen, and Yu Shrike Zhang**

Cancer tissue engineering has remained challenging due to the limitations of the conventional biofabrication techniques to model the complex tumor microenvironment. Here, the utilization of a sacrificial bioprinting strategy is reported to generate the biomimetic mammary duct-like structure within a hydrogel matrix, which is further populated with breast cancer cells, to model the genesis of ductal carcinoma and its subsequent outward invasion. This bioprinted mammary ductal carcinoma model provides a proof-of-concept demonstration of the value of using the sacrificial bioprinting technique for engineering biologically relevant cancer models, which may be possibly extended to other cancer types where duct-like structures are involved.

1. Introduction

Cancer is among the leading causes of death around the world.[1] In particular, breast cancer is one of the prevalent cancer types among Americans, resulting in a likelihood of approximately one in eight (12%) women in the United States developing invasive breast cancer (e.g., invasive ductal carcinoma [IDC]) during their lifetime.[2] Carcinoma in situ, including >85% ductal carcinoma in situ (DCIS),[3] although not considered life-threatening and only accounts for a small percentage of deaths, has been shown to increase the risk of developing invasive breast cancers at later stages.[3,4]

Although improved breast cancer survival has been achieved, current therapies relying on chemotherapy and radiation often lead to disparity in effectiveness and a high cost of cancer care.[5–15] At present, the selection of a drug for a specific cancer patient, or precision cancer medicine, relies on molecular and genetic profiling,[16,17] which, however, often does not translate into a successful clinical outcome and may provide clinical benefit in only selected patients.[18–20] In recent years, evidence has shown that patient-derived xenograft (PDX) animal models have a relatively good predictive power for personalized cancer drug screening, but they are limited by the high costs due to high failure rates and lengthy times needed for establishing these models.[21–23]

In comparison, conventional in vitro cancer cell culture studies are cost-effective, fast, and enable high throughput. However, they have not been able to model the complex physiology due to the oversimplified structures that they represent and they often fail to predict human responses towards therapeutic compounds.[24,25] Therefore, there is a need for the development of biomimetic in vitro cancer models that reproduce the important and complex characteristics of their in vivo counterparts.[25] These models may, to a certain degree, overcome some limitations of the PDX models as well as bridge the gap in the deficiencies of conventional in vitro models of two-dimensional (2D) cell cultures. As such, further improvements and validations of these biomimetic in vitro cancer models are anticipated to facilitate precision cancer therapy and lower the costs of pharmaceutical testing.[25–32]

To date, breast cancer has been successfully modeled in various ways,[33] ranging from the use of porous polymer scaffolds[34] and embedment in hydrogel matrices[35] to the application of microfabricated devices.[36] Nevertheless, rarely have there been

M. Duchamp, T. Liu, A. M. van Genderen, V. Kappings, Prof. Y. S. Zhang
Division of Engineering in Medicine
Department of Medicine
Brigham and Women's Hospital
Harvard Medical School
Cambridge, MA 02139, USA
E-mail: yszhang@research.bwh.harvard.edu

M. Duchamp
Department of Bioengineering
École Polytechnique Fédérale de Lausanne
Lausanne 1015, Switzerland

T. Liu
Center of Clinical Experiments
Changhai Hospital, Second Military Medical University
Shanghai 200433, P. R. China

A. M. van Genderen
Division of Pharmacology
Utrecht Institute for Pharmaceutical Sciences, Utrecht University
3584 CG, Utrecht, The Netherlands

V. Kappings
Institute of Toxicology and Genetics
Karlsruhe Institute of Technology
76131, Karlsruhe, Germany

Prof. R. Oklu
Division of Vascular and Interventional Radiology
Mayo Clinic
Scottsdale, AZ 85259, USA

Prof. L. W. Ellisen
Massachusetts General Hospital Cancer Center
Harvard Medical School
Boston, MA 02114, USA

DOI: 10.1002/biot.201700703

examples of including mammary duct-like structures, which are locations where ductal carcinoma initiates, in these in vitro models. One relevant report took advantage of microfabricated microchannels in a polydimethylsiloxane (PDMS) chip device to form biomimetic mammary ducts with seeded human mammary epithelial cells for screening of theranostics.[32] The major limitation with this model lies in the inability of the silicone elastomer to reproduce the extracellular matrix (ECM) properties of the mammary ducts in vivo, hence prohibiting studies pertaining to cell–matrix interactions.

Here, we demonstrate the design of an in vitro mammary ductal carcinoma model that has the potential to be employed in the recapitulation of the in vivo ductal carcinoma microenvironment. Specifically, we have utilized a sacrificial bioprinting strategy, where hollow microchannels of a desired size and morphology can be conveniently fabricated in a hydrogel matrix, leading to the high-fidelity generation of the mammary duct-like structure in an ECM-like microenvironment. By populating the microchannel with breast cancer cells, a ductal carcinoma model could be subsequently constructed, in which the cells were observed to first populate the interior surface of the microchannel and then proliferate within the ducts, followed by invasion into the surrounding matrix upon confluency.

2. Experimental Section

2.1. Materials

Chemicals including gelatin, methacrylic anhydride, photoinitiator Irgacure 2959, and agarose were purchased from Sigma-Aldrich (St. Louis, MO, USA) and used without further purification. Gelatin methacryloyl (GelMA) was synthesized according to our established protocol.[37–45] Briefly, gelatin was dissolved in phosphate-buffered saline ([PBS]; Thermo Fisher Scientific, Waltham, MA, USA) over a 2-hour course under constant stirring to yield a 5 wt% gelatin solution. To modify with methacryloyl groups, a volume corresponding to 4 vol% of the gelatin solution of methacrylic anhydride was added gradually to the solution and subsequently incubated and stirred for one hour at 37 °C and 500 rpm. Two volumes of preheated PBS were then added to the solution and the mixture was dialyzed for 7 days against deionized water. After dialysis, the obtained GelMA solution was filtered, freeze-dried, and stored at −20 °C until use. GelMA used in this work had a methacryloyl substitution degree of 80–85%, determined by ^{1}H NMR analysis as previously reported by us.[46]

2.2. Sacrificial Bioprinting

Sacrificial bioprinting was performed using an Organovo NovoGen MMX bioprinter (Organovo, San Diego, CA, USA) by modifying established protocols,[43,47] where agarose was used as the sacrificial material to allow for convenient physical extraction. In a typical procedure, an agarose solution (8 wt% in PBS) heated at 80 °C was loaded into the glass capillary (500 μm in diameter) of the printhead. The capillary was then immersed in a cold PBS at 4 °C for 10 s to induce the gelation of the agarose solution within the capillary. To extrude the gelled agarose microfiber, the stainless-steel piston was pushed down through the capillary against the agarose while a custom-written script coordinated the movement of the stage and the printhead to bioprint the agarose microfiber in a predefined shape. This agarose microfiber was placed on a piece of physically gelled GelMA hydrogel (5 wt% and 0.5 wt% photoinitiator in PBS) in a PDMS container with a dimension of $5 \times 10 \times 5$ mm^3 ($W \times L \times H$), following which another layer of GelMA of the same composition was covered on top and UV-crosslinked for 30 s from each side of the hydrogel construct. The GelMA block containing the bioprinted agarose construct was then retrieved from the PDMS holder and the microfiber was selectively removed by manual extraction to form the hollow duct-like microchannels. The samples were subsequently equilibrated and stored in PBS until further use.

2.3. Cell Culture and Seeding

MCF-7 cells (IDC, HTB-22; ATCC, Manassas, VA, USA) that belong to the Luminal A (estrogen receptor-positive, progesterone receptor-positive, human epidermal growth factor receptor 2-negative) classification were used in the current study. This cell line was chosen as they show a patchy/clustered epithelial morphology with relatively low invasiveness, which allows for longer-term characterization of the bioprinted duct-like microchannels. The cells were maintained in Dulbecco's modified Eagle medium, supplemented with 10 vol% fetal bovine serum and 1 vol% penicillin–streptomycin (all from Thermo Fisher Scientific). For seeding, the MCF-7 cells were dissociated from the flask and resuspended in the culture medium at a density of 5×10^6 cells mL^{-1}. This suspension was slowly injected into the microchannel in the GelMA hydrogel construct using an inserted syringe needle. Once the microchannel was filled with the cell suspension, the construct was left in a Petri dish in an incubator for 30 min on each side without media to prevent the outflow of the cells from the microchannels. After cell attachment onto the inner surface of the microchannel, media were gently flushed using a syringe needle to wash away the nonadherent cells. The cell-laden GelMA hydrogel construct was then transferred to a six-well plate filled with culture medium and maintained in an incubator set at 37 °C and 5 vol% CO_2 for subsequent culture.

2.4. Cellular Characterizations

Percentage of cell coverage and average invasion distance were measured using ImageJ (National Institutes of Health, Bethesda, MD, USA) on bright-field projection images as previously reported.[48]

Cell viability was measured using a LIVE/DEAD Viability/Cytotoxicity Kit (L-3224; Thermo Fisher Scientific) according to the manufacturer's instructions. Briefly, the hydrogel constructs were washed once with PBS after medium removal. Then, a working solution of 2 μL mL^{-1} of ethidium homodimer-1 and 0.5 μL mL^{-1} of calcein AM in PBS was prepared and 300 μL of this solution was placed on top of each construct. The hydrogel constructs were subsequently incubated at 37 °C for 15 min.

Afterwards, the constructs were washed twice with PBS and resuspended in PBS for imaging. Cell viability was quantified by counting the numbers of live and dead cells using ImageJ.

Cell metabolic activities were measured using the PrestoBlue Cell Viability Reagent (A13262; Thermo Fisher Scientific) according to the manufacturer's instructions. The hydrogel constructs were washed once with PBS after medium removal, and then a working solution of 9:1 culture medium to the reagent was placed in each well (24-well plate), incubated for 2 h at 37 °C, followed by retrieval and reading using a spectrophotometer (excitation: 570 nm, emission: 600 nm).

Cell morphology was assessed via F-actin/nuclei staining. After fixation with 4 vol% paraformaldehyde (Electron Microscopy Sciences, Hatfield, PA, USA) and permeation with 0.1% Triton X-100 (Sigma-Aldrich), F-actin and nuclei were stained using Alexa 488-phalloidin (Thermo Fisher Scientific) and 4′,6-diamidino-2-phenylindole ([DAPI]; Thermo Fisher Scientific), respectively, according to the manufacturer's instructions. Alexa 488-phalloidin was diluted at a ratio of 1:40 v/v in 0.1% bovine serum albumin ([BSA]; Thermo Fisher Scientific) in PBS. Each construct after fixation, permeation, and blocking was washed with PBS three times for 5 minutes. Subsequently, 300 μL of the prepared phalloidin staining solution was placed on each construct and allowed to incubate for 45 min at 37 °C. In a similar manner, a working solution of DAPI diluted at 1:1000 v/v in PBS was prepared. Following F-actin staining, the constructs were washed once with PBS and then stained with 300 μL of working DAPI solution incubated at 37 °C for 5 min. The constructs were finally washed once with PBS and resuspended in the same for storage and imaging.

Basement membrane protein collagen type IV was characterized using immunostaining with anticollagen type IV (ab6586; Abcam, Cambridge, MA, USA) antibody, and possible epithelial–mesenchymal transition (EMT) was examined by immunostaining with anti-E-cadherin (ab40772; Abcam) and anti-N-cadherin (ab98952; Abcam) antibodies. Alexa 594-conjugated secondary antibodies (goat anti-rabbit immunoglobulin G [IgG]; Thermo Fisher Scientific) and Alexa 488-conjugated secondary antibodies (goat anti-mouse IgG; Thermo Fisher Scientific) were used to visualize the primary antibodies. The devices were washed three times with PBS, fixed with 4% w/v paraformaldehyde in PBS for 15 min at 37 °C, followed by three PBS washes at room temperature and permeation with 0.1% v/v Triton X-100 for 20 min at 37 °C. The samples were blocked using 5% v/v goat serum for 30 min at room temperature and then incubated overnight (>16 h) at 4 °C with primary antibodies diluted in 5% v/v goat serum at a ratio 1:100 v/v. This step was followed by three washes using PBS and then incubation with the desired secondary antibodies in 5% v/v goat serum for two hours at room temperature at a 1:200 v/v ratio. The stained samples were imaged using a Zeiss Confocal Microscope (LSM 880 with Airyscan; Carl Zeiss, Thornwood, NY, USA) and reconstructed using ImageJ.

2.5. Statistical Analyses

At least five randomly distributed images were taken per sample for analysis. The sample sizes used for quantifications were three in all groups. Data were presented as means ± standard deviations. Statistical analyses were performed using Students' *t*-test by GraphPad Prism 6 or Origin 8.

3. Results and Discussions

3.1. The Sacrificial Bioprinting Process

The sacrificial bioprinting procedure is divided into six different steps (**Figure 1**A). In the first step, the PDMS mold is filled with a layer of GelMA and cooled to room temperature (21 °C) to achieve physical gelation.[49] An agarose microfiber is then extruded onto this GelMA layer using a bioprinter, followed by casting of another layer of GelMA and subsequent photocrosslinking of the entire hydrogel construct (Figure 1B). In the final steps, the agarose microfiber is gently removed using physical force from the GelMA construct to induce the formation of the reverse replica of the microchannel, i.e., the hollow microchannel (Figure 1C,D). This microchannel within the hydrogel can be further seeded with cells to endow it with biological functions. Through the programming of the bioprinter movement, single or multiple microchannels of different geometries and diameters may be generated within a hydrogel matrix to model the mammary ducts of different sizes, tortuosity, and branching. Perfusion of the microchannels can also be realized by fitting external tubing into the microchannels when necessary (Figure 1E).

Sacrificial bioprinting has been widely adopted in engineering tubular tissues, such as the vasculature,[47,50–52] and it has been shown in other models (kidney and gut) that curvature can be crucial for the formation of monolayers and epithelial barrier functions.[53,54] Consequently, we anticipate that our topologically relevant ductal carcinoma model would have similar advantages, although it is not the focus of current study and will be systematically investigated and reported in future publications. The bioprinted sacrificial material can be from various sources, ranging from carbohydrate glass microfibers that may be removed by dissolution in the culture medium[52] to temperature-sensitive materials that may be removed by liquefaction upon decrease (e.g., Pluronic[50,55]) or increase (e.g., gelatin[51]) of ambient temperature. In comparison, the use of agarose allows easy physical extraction of the bioprinted microfibers from the surrounding hydrogel matrix,[47] which is typically faster than when using other materials, potentially leading to reduced adverse effects on the cells embedded in the constructs as no additional treatments are needed for the removal. In addition, it should be noted that it is straightforward to dissociate desired portions of a matrix using proteases such as collagenase to retrieve specific cell populations and extract RNA out of the system using the Trizol reagent (or similar) to perform molecular interrogations, as needed.

3.2. Construction of the Mammary Ductal Carcinoma Model

In particular, we chose GelMA as the matrix component for our proof-of-principle studies because this cost-effective biomacromolecule containing mixed molecular weights degraded from collagen allows for rapid gelation upon temperature change and

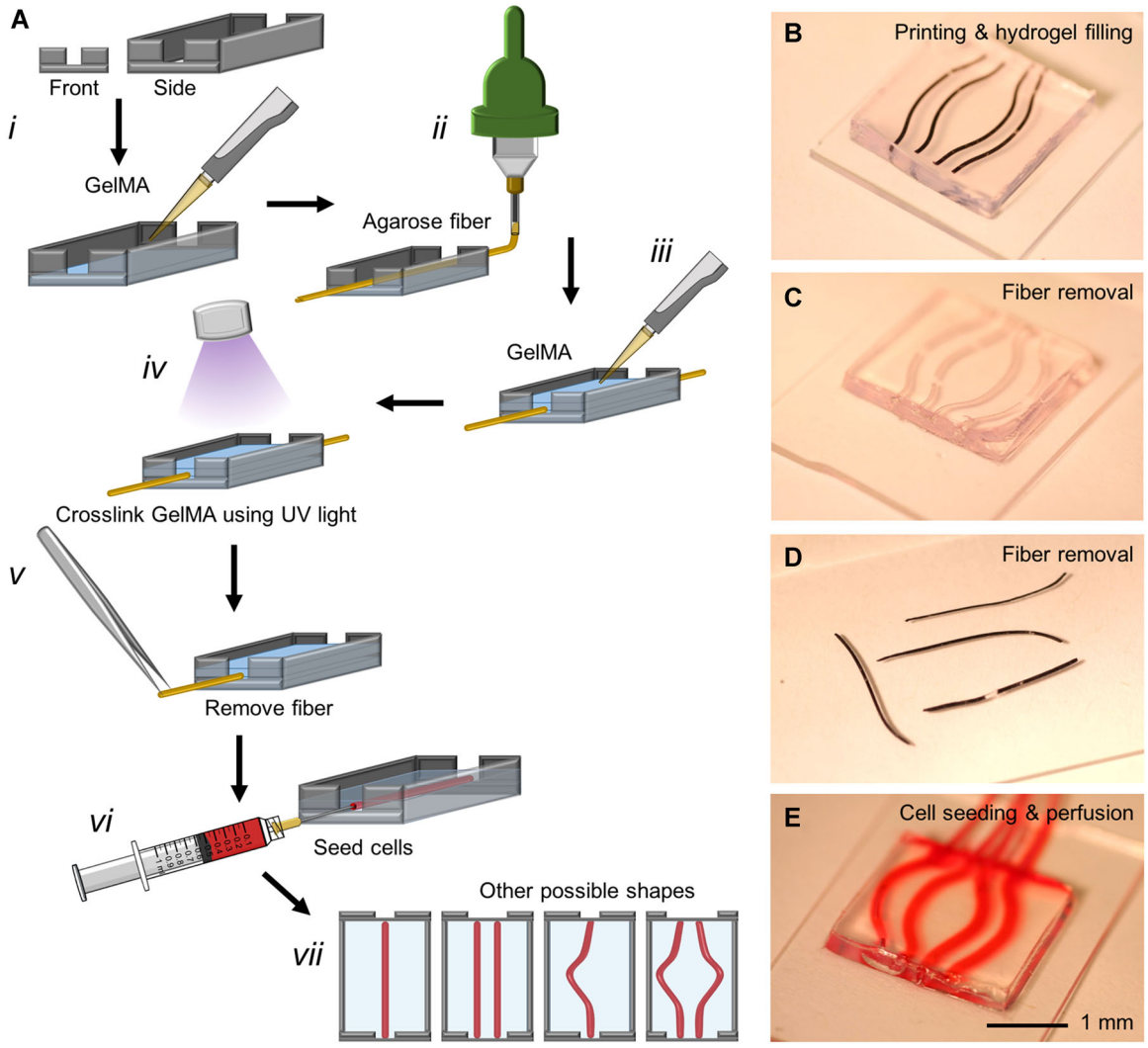

Figure 1. Sacrificial bioprinting of hydrogel-embedded hollow microchannels. A) Schematics showing a typical procedure of the sacrificial bioprinting process: (i) deposition of a thin layer of GelMA at the bottom of the mold; (ii) bioprinting of agarose microfiber(s) into the mold; (iii) casting of the mold with GelMA prepolymer; (iv) induction of gelation using photocrosslinking; (v) extraction of the agarose microfiber(s) manually or using mild vacuum; (vi) seeding of the mammary ductal carcinoma cells on the interior surface(s) of the bioprinted microchannel(s); and (vii) a variety of different shapes mimicking the mammary ducts can be generated using such a method. B–E) Photographs showing the bioprinted agarose microfibers in the cast GelMA hydrogel, microchannels formed after removal of the agarose microfibers, the removed agarose microfibers, and perfusion of the microchannels.

enables convenient chemical crosslinking under proper light illumination.[46,49,53,54,56] Additionally, GelMA has been demonstrated to be compatible with a wide range of cells due to the intrinsic cell-adhesive moieties contained in the backbone of the macromolecules.[46,53,54] It was also recently used in cancer tissue engineering where several cancer cell types including breast cancer cells showed strong growth potential within the hydrogel matrices made from GelMA.[57,58]

Indeed, upon seeding, the MCF-7 cells attached to the interior surface of the microchannel possibly due to the interaction of the integrins with the RGD peptides in GelMA molecules (**Figure 2**A). The cells continued to proliferate within the microchannel over a course of 2 weeks (Figure 2B–D). Upon confluency at day 19 of culture (Figure 2E), the MCF-7 cells began to invade and sprout into the surrounding hydrogel matrix through up to 24 days of evaluation (Figure 2F). The viability of the cells remained stable, with a slightly decreased rate at the later stage of culture (Figure 2G). Increased nutrient and oxygen consumption in the medium by the cells might play a role in this decreased viability rate. Interestingly, while most cells started to invade into the GelMA matrix after day 19 of culture when the entire microchannel was covered, there were local confluent regions even at earlier times that resulted in the sprouting of the MCF-7 cells (Figure 2C–F,H). Such an observation suggested the biomimetic property of our model to reproduce some of the ductal carcinoma behaviors including proliferation of the cancer cells in local regions, as well as signs of invasion into the space outside the mammary duct area.[55,59–61]

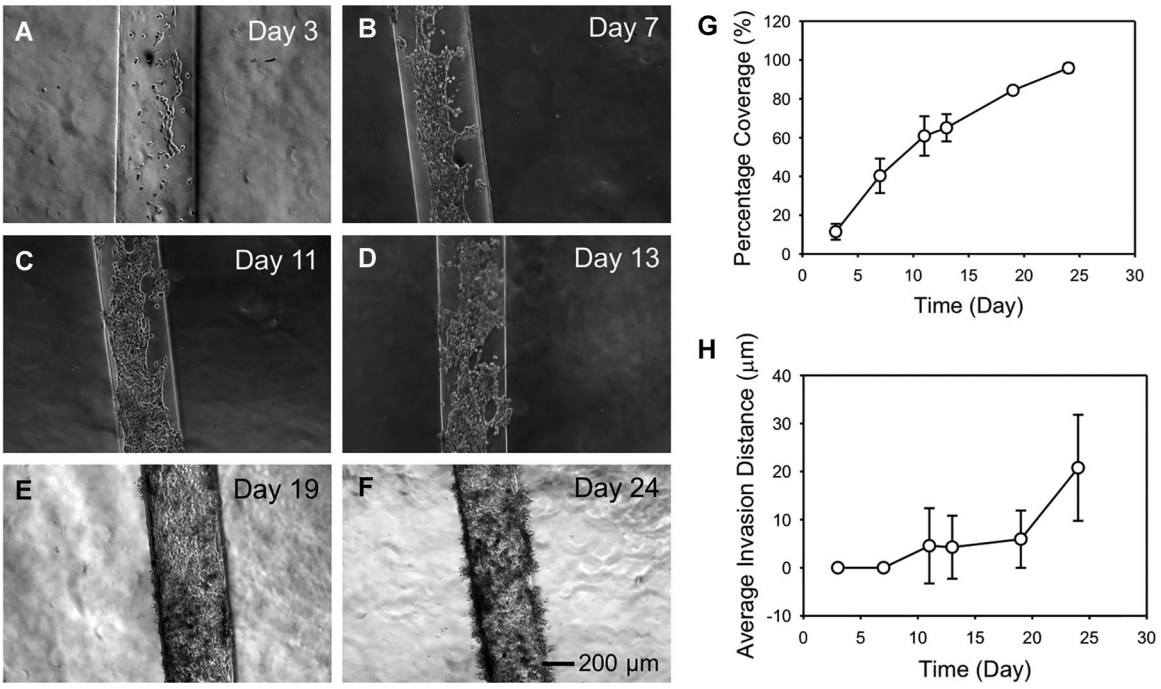

Figure 2. Proliferation of the seeded MCF-7 cells within the bioprinted mammary duct-like microchannel. A–F) Optical micrographs showing the proliferation of the cells over a culture period of 24 days. G) Quantification of percentage coverage of the cells. H) Quantification of the invasion distance of the cells into the surrounding matrix.

Although GelMA is shown here as a possible ECM for the ductal carcinoma model that was previously demonstrated to support cancer cell growth,[62] the GelMA hydrogel is obviously lacking many native ECM characteristics. In the future, various ECM components could be incorporated into the hydrogel, such as fibronectin, collagens, laminins, proteoglycans, and matricellular proteins. This will most likely improve the resemblance of the ECM to the physiological situation of the ductal carcinoma tumor, and might also stimulate the proliferative and migratory properties of the MCF-7 cells.[63] In fact, it was also shown before that, the use of stage-matched tumor matrix proteins would facilitate phenotype preservation in ex vivo cultures of tumor biopsies.[64,65]

3.3. Characterization of the Mammary Ductal Carcinoma Model

The bioprinted ductal carcinoma model was also subjected to biochemical analyses to characterize key behaviors of the cells including proliferation and invasion. Viability assays indicated the ability of the MCF-7 cells to remain viable within the microchannels even after 24 days of culture (**Figure 3**A). In fact, the viability of the MCF-7 cells in the microchannels exceeded >85% throughout the entire culture period with negligible variations (Figure 3B), indicating the favorable microenvironment that the bioprinted hydrogel microchannels had provided for these cells, as well as the adequate diffusion of nutrients and oxygen through the GelMA construct and through the microchannels. MCF-7 cell proliferation was significantly increased at day 7 of culture compared to day 3 and the proliferation of the cells gradually slowed down afterwards (Figure 3C).

F-actin staining for MCF-7 cells within the microchannels was further performed after 7, 14, and 24 days of culture (**Figure 4**A–C). The staining at day 24 of culture clearly revealed a heterogeneous cell distribution, where those in the upper region of the specific microchannel invaded into the surrounding matrix much faster than the cells in the lower region of the same microchannel (Figure 4C). Not only did the cells invade into the surrounding matrix, the culture also led to their inward aggregation (Figure 3C), resembling the characteristics of late-stage DCIS and early-stage IDC.[55,59–61] Orthogonal views of the same microchannels also illustrated the same process, where the cells gradually proliferated in the microchannel and invaded into the surrounding matrix along with inward growth (Figure 4D–F). The heterogeneous distribution of MCF-7 cells could be partially attributed to the seeding process, where cell suspension at a very high density was used for seeding to ensure cell adhesion, followed by a subsequent wash of the nonadherent cells. This might have induced slight differences in cell density at different locations along the microchannel at the initial time point (Figure 4D), which, with prolonged culture, might have gone through a remodeling process to occupy the entire microchannels (Figure 4E) and eventually evolved into more pronounced inhomogeneous structures (Figure 4F). However, such heterogeneity of the MCF-7 cells also primitively resembled the intratumor heterogeneity in human cancers, which have been the main challenge associated with efficient therapeutic options.[8,66,67]

Deposition of basement membrane molecules is another feature of these breast cancer cells that are epithelial in nature; basement membrane molecules are secreted mainly by myoepithelial cells but not by luminal epithelial cells. As

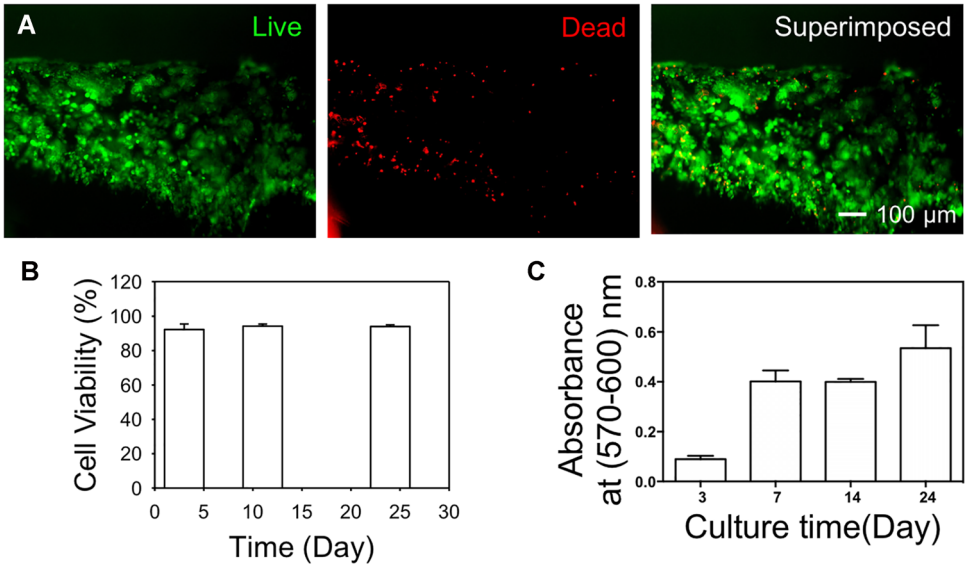

Figure 3. Characterizations of the bioprinted ductal carcinoma model. A) Live/dead staining of MCF-7 cells in the microchannel after 24 days of culture. B) Quantified staining of cells at 3, 11, and 24 days of culture. C) Quantification of metabolic activities of the cells on days 3, 7, 14, and 24 of culture using the PrestoBlue assay ($*p < 0.05$, $**p < 0.01$, $***p < 0.001$; $n = 3$).

MCF-7 cells retain numerous characteristics of the luminal epithelial cells, they have been reported to secrete some of the basement membrane main constituents (e.g., collagen IV) but not others (e.g., laminins).[68] To this end, we further stained our MCF-7 cell-populated, bioprinted mammary duct-like structure for basement membrane molecules including collage type IV and laminin. Consistent with the literature, our staining results clearly showed strong expression of collagen type IV by

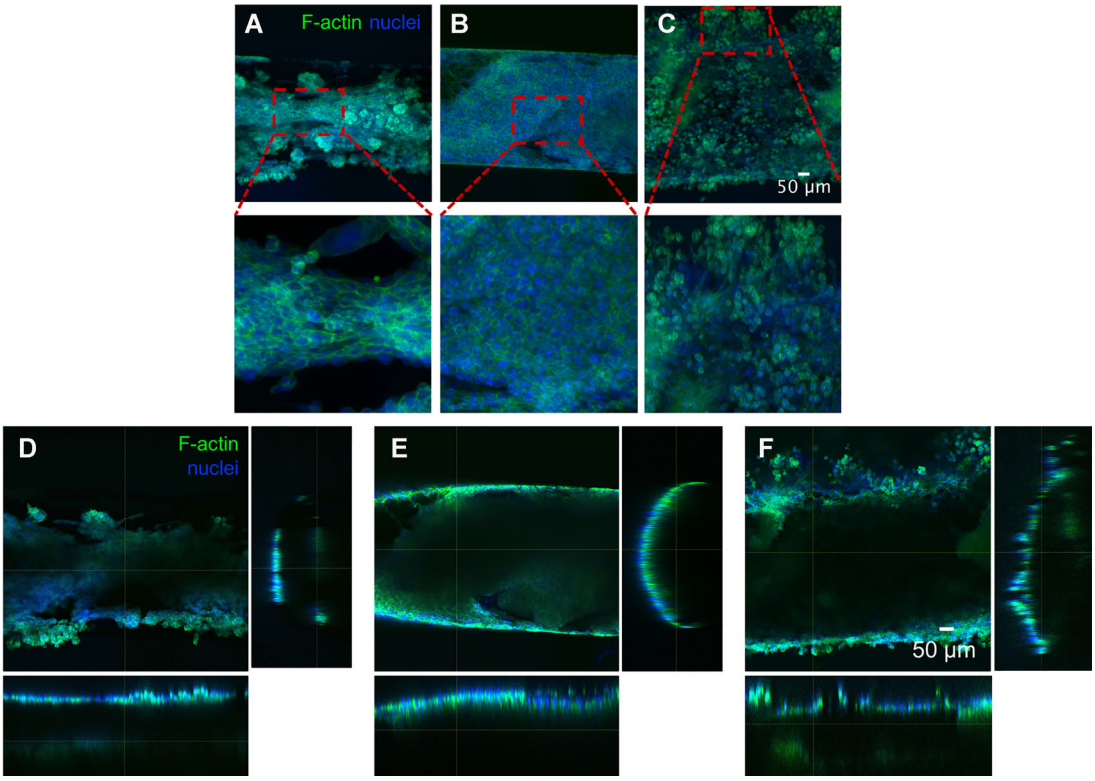

Figure 4. Confocal images of the bioprinted ductal carcinoma model. A–C) Projection views of the microchannel region populated by MCF-7 cells stained for F-acting (green) and nuclei (blue) at 7, 14, and 24 days of culture, respectively. D–F) Orthogonal views of the respective samples shown in (A–C).

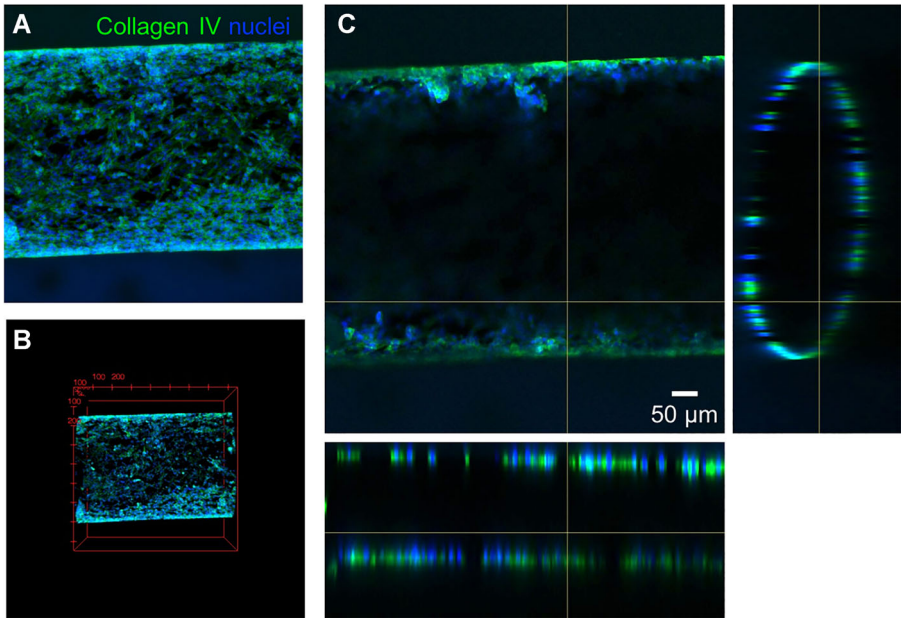

Figure 5. Confocal images of the bioprinted ductal carcinoma model after 14 days of culture. A) Projection, B) reconstruction, and C) orthogonal views showing deposition of collagen IV (green) by the MCF-7 cells. Nuclei were counterstained in blue.

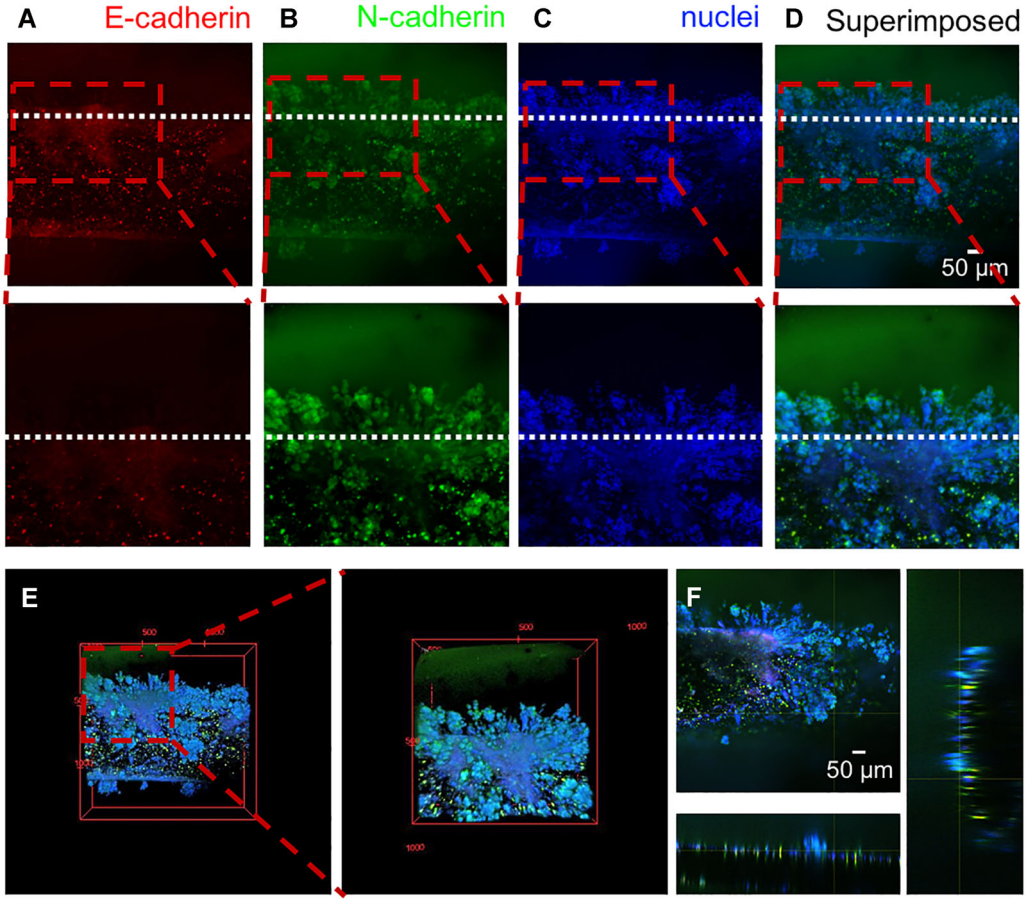

Figure 6. Confocal images showing E-cadherin and N-cadherin expressions of MCF-7 cells in the bioprinted ductal carcinoma model after 24 days of culture. A–D) Projection images showing E-cadherin (red), N-cadherin (green), and nuclei (blue) staining. White dotted lines indicate the boundary of the microchannel. E,F) Reconstruction images and orthogonal views of the same sample, respectively.

the MCF-7 cells at day 14 (**Figure 5**). At a later time point where the cells already started to invade into the surrounding matrix, more pronounced collagen IV deposition was mainly found in the regions where the cells overproliferated (Figure S1, Supporting Information). In contrast, laminin secretion was not detected (Figure S2, Supporting Information).

As anticipated, the changes in expression profiles of the MCF-7 cells in the bioprinted mammary duct-like microchannel suggested that these cells might have lost their epithelial phenotype since repression of E-cadherin and induction of N-cadherin were moderately increased at the locations of invasion throughout the 24-day culture period (**Figure 6**). In most metazoans, epithelial sheets can be reversibly or irreversibly converted into mesenchymal cell by EMT.[69] The biomarker expression changes of the invading cells, that is, loss of E-cadherin and induction of N-cadherin, indicated that the cells underwent a developmental switch from epithelial phenotypes to cancer progression. However, whether the cells have entered the EMT status would need further investigations through meticulous genetic profiling.

4. Conclusions

In summary, this technical report has demonstrated our successful adaptation of the sacrificial bioprinting strategy in engineering biomimetic cancer models, specifically, a mammary ductal carcinoma model. By seeding breast cancer cells into microchannels mimicking the mammary ducts, these cells exhibited several characteristic behaviors potentially similar to those of ductal carcinoma, including proliferation, invasion into the surrounding matrix, heterogeneous structures, and deposition of basement membrane molecules. While this model remains preliminary in nature, we believe that it represents a significant advancement in using engineering technologies to model cancer tissues in a 3D manner, in which cancer cells have the potential to reproduce the basic morphological and functional features of their in vivo counterparts. It is also anticipated that this proof-of-concept technology will enable the incorporation of patient-derived cells to realize individualized drug selection in the future. In addition, this bioprinting strategy is a general one that might be extended to other cancer types where duct-like structures are involved.

Supporting Information

Supporting Information is available from the Wiley Online Library or from the author.

Acknowledgements

M.D. and T.L. contributed equally to this work. Y.S.Z. acknowledges funds from the National Institutes of Health (K99CA201603, R00CA201603, R21EB025270, R21EB026175, R01EB028143), the Brigham Research Institute, the Lush Prize, and the New England Anti-Vivisection Society (NEAVS).

Conflict of Interest

The authors declare no conflict of interest.

Keywords

bioprinting, breast cancer, cancer model, ductal carcinoma, hydrogel

Received: November 16, 2017
Revised: March 15, 2019
Published online: May 27, 2019

[1] R. L. Siegel, K. D. Miller, A. Jemal, *CA Cancer J. Clin.* **2018**, *68*, 7.
[2] S. B. Giordano, W. Gradishar, *Curr. Opin. Obstet. Gynecol.* **2017**, *29*, 12.
[3] J. Heymach, L. Krilov, A. Alberg, N. Baxter, S. M. Chang, R. B. Corcoran, W. Dale, A. DeMichele, C. S. Magid Diefenbach, R. Dreicer, A. S. Epstein, M. L. Gillison, D. L. Graham, J. Jones, A. H. Ko, A. M. Lopez, R. G. Maki, C. Rodriguez-Galindo, R. L. Schilsky, M. Sznol, S. N. Westin, H. Burstein, *J. Clin. Oncol.* **2018**, *36*, 1020.
[4] C. E. DeSantis, J. Ma, A. Goding Sauer, L. A. Newman, A. Jemal, *CA Cancer J. Clin.* **2017**, *67*, 439.
[5] L. Tabár, S. W. Duffy, B. Vitak, H. H. Chen, T. C. Prevost, *Cancer* **1999**, *86*, 449.
[6] H. Kitano, *Nat. Rev. Cancer* **2004**, *4*, 227.
[7] M. Shipitsin, L. L. Campbell, P. Argani, S. Weremowicz, N. Bloushtain-Qimron, J. Yao, T. Nikolskaya, T. Serebryiskaya, R. Beroukhim, M. Hu, M. K. Halushka, S. Sukumar, L. M. Parker, K. S. Anderson, L. N. Harris, J. E. Garber, A. L. Richardson, S. J. Schnitt, Y. Nikolsky, R. S. Gelman, K. Polyak, *Cancer Cell* **2007**, *11*, 259.
[8] K. Polyak, *J. Clin. Invest.* **2011**, *121*, 3786.
[9] M. Gerlinger, A. J. Rowan, S. Horswell, J. Larkin, D. Endesfelder, E. Gronroos, P. Martinez, N. Matthews, A. Stewart, P. Tarpey, I. Varela, B. Phillimore, S. Begum, N. Q. McDonald, A. Butler, D. Jones, K. Raine, C. Latimer, C. R. Santos, M. Nohadani, A. C. Eklund, B. Spencer-Dene, G. Clark, L. Pickering, G. Stamp, M. Gore, Z. Szallasi, J. Downward, P. A. Futreal, C. Swanton, *New Engl. J. Med.* **2012**, *366*, 883.
[10] H. Seol, H. J. Lee, Y. Choi, H. E. Lee, Y. J. Kim, J. H. Kim, E. Kang, S.-W. Kim, S. Y. Park, *Mod. Pathol.* **2012**, *25*, 938.
[11] C. Swanton, *Cancer Res.* **2012**, *72*, 4875.
[12] T. A. Yap, M. Gerlinger, P. A. Futreal, L. Pusztai, C. Swanton, *Sci. Transl. Med.* **2012**, *4*, 127.
[13] R. A. Burrell, N. Mcgranahan, J. Bartek, C. Swanton, *Nature* **2013**, *501*, 338.
[14] T. N. Chirikos, *Cancer Control* **2002**, *9*, 59.
[15] O. Ginsburg, F. Bray, M. P. Coleman, V. Vanderpuye, A. Eniu, S. R. Kotha, M. Sarker, T. T. Huong, C. Allemani, A. Dvaladze, J. Gralow, K. Yeates, C. Taylor, N. Oomman, S. Krishnan, R. Sullivan, D. Kombe, M. M. Blas, G. Parham, N. Kassami, L. Conteh, *Lancet* **2017**, *389*, 847.
[16] S. Siena, A. Sartore-Bianchi, F. Di Nicolantonio, J. Balfour, A. Bardelli, *J. Natl. Cancer Inst.* **2009**, *101*, 1308.
[17] L. J. Van 't veer, R. Bernards, *Nature* **2008**, *452*, 564.
[18] D. J. Samson, J. Seidenfeld, K. Ziegler, N. Aronson, *J. Clin. Oncol.* **2004**, *22*, 3618.
[19] J. Barretina, G. Caponigro, N. Stransky, K. Venkatesan, A. A. Margolin, S. Kim, C. J. Wilson, J. Lehár, G. V. Kryukov, D. Sonkin, A. Reddy, M. Liu, L. Murray, M. F. Berger, J. E. Monahan, P. Morais, J. Meltzer, A. Korejwa, J. Jané-Valbuena, F. A. Mapa, J. Thibault, E. Bric-Furlong, P. Raman, A. Shipway, I. H. Engels, J. Cheng, G. K. Yu, J. Yu, P. Aspesi, M. de Silva, K. Jagtap, M. D. Jones, L. Wang, C. Hatton, E. Palescandolo, S. Gupta, S. Mahan, et al., *Nature* **2012**, *483*, 603.
[20] D. Cunningham, Y. Humblet, S. Siena, D. Khayat, H. Bleiberg, A. Santoro, D. Bets, M. Mueser, A. Harstrick, C. Verslype, I. Chau, E. Van Cutsem, *New Engl. J. Med.* **2004**, *351*, 337.
[21] S. Y. C. Choi, D. Lin, P. W. Gout, C. C. Collins, Y. Xu, Y. Wang, *Adv. Drug Del. Rev.* **2014**, *79-80*, 222.
[22] S. Aparicio, M. Hidalgo, A. L. Kung, *Nat. Rev. Cancer* **2015**, *15*, 311.

[23] A. T. Byrne, D. G. Alférez, F. Amant, D. Annibali, J. Arribas, A. V. Biankin, A. Bruna, E. Budinská, C. Caldas, D. K. Chang, R. B. Clarke, H. Clevers, G. Coukos, V. Dangles-Marie, S. G. Eckhardt, E. Gonzalez-Suarez, E. Hermans, M. Hidalgo, M. A. Jarzabek, S. De Jong, J. Jonkers, K. Kemper, L. Lanfrancone, G. M. Mælandsmo, E. Marangoni, J.-C. Marine, E. Medico, J. H. Norum, H. G. Palmer, D. S. Peeper, P. G. Pelicci, A. Piris-Gimenez, S. Roman-Roman, O. M. Rueda, J. Seoane, V. Serra, et al., *Nat. Rev. Cancer* **2017**, *17*, 254.
[24] Y. S. Zhang, M. Duchamp, R. Oklu, L. W. Ellisen, R. Langer, A. Khademhosseini, *ACS Biomater. Sci. Eng.* **2016**, *2*, 1710.
[25] Y. S. Zhang, Y.-N. Zhang, W. Zhang, *Drug Discovery* **2017**, *22*, 1392.
[26] J. A. Hickman, R. Graeser, R. De Hoogt, S. Vidic, C. Brito, M. Gutekunst, H. van der Kuip, IMI PREDECT Consortium, *Biotechnol. J.* **2014**, *9*, 1115.
[27] B. R. Seo, P. Delnero, C. Fischbach, *Adv. Drug Del. Rev.* **2014**, *69–70*, 205.
[28] K. E. Sung, D. J. Beebe, *Adv. Drug Del. Rev.* **2014**, *79–80*, 68.
[29] C. Unger, N. Kramer, A. Walzl, M. Scherzer, M. Hengstschläger, H. Dolznig, *Adv. Drug Del. Rev.* **2014**, *79–80*, 50.
[30] L. L. Bischel, D. J. Beebe, K. E. Sung, *BMC Cancer* **2015**, *15*, 12.
[31] Y. Choi, E. Hyun, J. Seo, C. Blundell, H. C. Kim, E. Lee, S. H. Lee, A. Moon, W. K. Moon, D. Huh, *Lab Chip* **2015**, *15*, 3350.
[32] M. M. G. Grafton, L. Wang, P.-A. Vidi, J. Leary, S. A. Lelièvre, *Integr. Biol.* **2011**, *3*, 451.
[33] P.-A. Vidi, J. F. Leary, S. A. Lelièvre, *Integr. Biol.* **2013**, *5*, 1110.
[34] C. Fischbach, R. Chen, T. Matsumoto, T. Schmelzle, J. S. Brugge, P. J. Polverini, D. J. Mooney, *Nat. Methods* **2007**, *4*, 855.
[35] P.-A. Vidi, M. J. Bissell, S. A. Lelièvre, *Methods Mol. Biol.* **2013**, *945*, 193.
[36] K. E. Sung, N. Yang, C. Pehlke, P. J. Keely, K. W. Eliceiri, A. Friedl, D. J. Beebe, *Integr. Biol.* **2011**, *3*, 439.
[37] Y. S. Zhang, J. Ribas, A. Nadhman, J. Aleman, Š. Selimović, S. C. Lesher-Perez, T. Wang, V. Manoharan, S. R. Shin, A. Damilano, N. Annabi, M. R. Dokmeci, S. Takayama, A. Khademhosseini, *Lab Chip* **2015**, *15*, 3661.
[38] N. S. Bhise, V. Manoharan, S. Massa, A. Tamayol, M. Ghaderi, M. Miscuglio, Q. Lang, Y. Shrike zhang, S. R. Shin, G. Calzone, N. Annabi, T. D. Shupe, C. E. Bishop, A. Atala, M. R. Dokmeci, A. Khademhosseini, *Biofabrication* **2016**, *8*, 014101.
[39] N. M. Oliveira, Y. S. Zhang, J. Ju, A.-Z. Chen, Y. Chen, S. R. Sonkusale, M. R. Dokmeci, R. L. Reis, J. F. Mano, A. Khademhosseini, *Chem. Mater.* **2016**, *28*, 3641.
[40] S. R. Shin, R. Farzad, A. Tamayol, V. Manoharan, P. Mostafalu, Y. S. Zhang, M. Akbari, S. M. Jung, D. Kim, M. Comotto, N. Annabi, F. E. Al-Hazmi, M. R. Dokmeci, A. Khademhosseini, *Adv. Mater.* **2016**, *28*, 3280.
[41] Y. S. Zhang, A. Arneri, S. Bersini, S.-R. Shin, K. Zhu, Z. Goli-Malekabadi, J. Aleman, C. Colosi, F. Busignani, V. Dell'erba, C. Bishop, T. Shupe, D. Demarchi, M. Moretti, M. Rasponi, M. R. Dokmeci, A. Atala, A. Khademhosseini, *Biomaterials* **2016**, *110*, 45.
[42] Y. S. Zhang, F. Busignani, J. Ribas, J. Aleman, T. N. Rodrigues, S. a M. Shaegh, S. Massa, C. B. Rossi, I. Taurino, S.-R. Shin, G. Calzone, G. M. Amaratunga, D. L. Chambers, S. Jabari, Y. Niu, V. Manoharan, M. R. Dokmeci, S. Carrara, D. Demarchi, A. Khademhosseini, , *Sci. Rep.* **2016**, *6*, 22237.
[43] Y. S. Zhang, F. Davoudi, P. Walch, A. Manbachi, X. Luo, V. Dell'Erba, A. K. Miri, H. Albadawi, A. Arneri, X. Li, X. Wang, M. R. Dokmeci, A. Khademhosseini, R. Oklu, *Lab Chip* **2016**, *16*, 4097.
[44] W. Liu, Y. S. Zhang, M. A. Heinrich, F. De Ferrari, H. L. Jang, S. M. Bakht, M. M. Alvarez, J. Yang, Y.-C. Li, G. Trujillo-De Santiago, A. K. Miri, K. Zhu, P. Khoshakhlagh, G. Prakash, H. Cheng, X. Guan, Z. Zhong, J. Ju, G. H. Zhu, X. Jin, S. R. Shin, M. R. Dokmeci, A. Khademhosseini, *Adv. Mater.* **2017**, *29*, 1604630.
[45] Y. S. Zhang, J. Aleman, S. R. Shin, T. Kilic, D. Kim, S. A. Mousavi Shaegh, S. Massa, R. Riahi, S. Chae, N. Hu, H. Avci, W. Zhang, A. Silvestri, A. Sanati Nezhad, A. Manbohi, F. De ferrari, A. Polini, G. Calzone, N. Shaikh, P. Alerasool, E. Budina, J. Kang, N. Bhise, J. Ribas, A. Pourmand, A. Skardal, T. Shupe, C. E. Bishop, M. R. Dokmeci, A. Atala, A. Khademhosseini, *Proc. Natl. Acad. Sci. U. S. A.* **2017**, *114*, E2293.
[46] K. Yue, X. Li, K. Schrobback, A. Sheikhi, N. Annabi, J. Leijten, W. Zhang, Y. S. Zhang, D. W. Hutmacher, T. J. Klein, A. Khademhosseini, *Biomaterials* **2017**, *139*, 163.
[47] L. E. Bertassoni, M. Cecconi, V. Manoharan, M. Nikkhah, J. Hjortnaes, A. L. Cristino, G. Barabaschi, D. Demarchi, M. R. Dokmeci, Y. Yang, A. Khademhosseini, *Lab Chip* **2014**, *14*, 2202.
[48] S. Li, L. R. Nih, H. Bachman, P. Fei, Y. Li, E. Nam, R. Dimatteo, S. T. Carmichael, T. H. Barker, T. Segura, *Nat. Mater.* **2017**, *16*, 953.
[49] W. Liu, M. A. Heinrich, Y. Zhou, A. Akpek, N. Hu, X. Liu, X. Guan, Z. Zhong, X. Jin, A. Khademhosseini, Y. S. Zhang, *Adv. Healthcare Mater.* **2017**, *6*, 1601451.
[50] D. B. Kolesky, R. L. Truby, A. S. Gladman, T. A. Busbee, K. A. Homan, J. A. Lewis, *Adv. Mater.* **2014**, *26*, 3124.
[51] V. K. Lee, D. Y. Kim, H. Ngo, Y. Lee, L. Seo, S.-S. Yoo, P. A. Vincent, G. Dai, *Biomaterials* **2014**, *35*, 8092.
[52] J. S. Miller, K. R. Stevens, M. T. Yang, B. M. Baker, D.-H. T. Nguyen, D. M. Cohen, E. Toro, A. A. Chen, P. A. Galie, X. Yu, R. Chaturvedi, S. N. Bhatia, C. S. Chen, *Nat. Mater.* **2012**, *11*, 768.
[53] K. Yue, G. Trujillo-De Santiago, M. M. Alvarez, A. Tamayol, N. Annabi, A. Khademhosseini, *Biomaterials* **2015**, *73*, 254.
[54] D. Loessner, C. Meinert, E. Kaemmerer, L. C. Martine, K. Yue, P. A. Levett, T. J. Klein, F. P. W. Melchels, A. Khademhosseini, D. W. Hutmacher, *Nat. Protocols* **2016**, *11*, 727.
[55] K. A. Homan, D. B. Kolesky, M. A. Skylar-Scott, J. Herrmann, H. Obuobi, A. Moisan, J. A. Lewis, *Sci. Rep.* **2016**, *6*, 34845.
[56] G. Ying, N. Jiang, C. Yu, Y. S. Zhang, *Bio-Des. Manuf.* **2018**, *1*, 215.
[57] E. Kaemmerer, F. P. W. Melchels, B. M. Holzapfel, T. Meckel, D. W. Hutmacher, D. Loessner, *Acta Biomater.* **2014**, *10*, 2551.
[58] I. Acerbi, L. Cassereau, I. Dean, Q. Shi, A. Au, C. Park, Y. Y. Chen, J. Liphardt, E. S. Hwang, V. M. Weaver, *Integr. Biol.* **2015**, *7*, 1120.
[59] V. Martinez, J. G. Azzopardi, *Histopathology* **1979**, *3*, 467.
[60] Z. Wei, G. Er-Li, Z. Yi-Li, Z. Qi, Z. Zhang-Yong, G. Gui-Long, C. Guo-Rong, Z. Hua-Min, H. Guan-Li, Z. Xiao-Hua, *World J. Surg. Oncol.* **2012**, *10*, 262.
[61] F. Farabegoli, M. H. Champeme, I. Bieche, D. Santini, C. Ceccarelli, M. Derenzini, R. Lidereau, *J. Pathol.* **2002**, *196*, 280.
[62] D. Sarrió, S. M. Rodriguez-Pinilla, D. Hardisson, A. Cano, G. Moreno-Bueno, J. Palacios, *Cancer Res.* **2008**, *68*, 989.
[63] A. Goldman, B. Majumder, A. Dhawan, S. Ravi, D. Goldman, M. Kohandel, PK. Majumder, S. Sengupta, *Nat. Commun.* **2015**, *6*, 6139.
[64] J. Insua-Rodríguez, T. Oskarsson, *Adv. Drug Deliv. Rev.* **2015**, *97*, 45.
[65] B. Majumder, U. Baraneedharan, S. Thiyagarajan, P. Radhakrishnan, H. Narasimha, M. Dhandapani, N Brijwani, D. D. Pinto, A. Prasath, B. U. Shanthappa, A. Thayakumar, R. Surendran, G. K. Babu, A. M. Shenoy, M. A. Kuriakose, G. Bergthold, P. Horowitz, M. Loda, R. Beroukhim, S. Agarwal, S. Sengupta, M. Sundaram, P. K. Majumder, *Nat. Commun.* **2015**, *6*, 6169.
[66] L. G. Martelotto, C. K. Ng, S. Piscuoglio, B. Weigelt, J. S. Reis-Filho, *Breast Cancer Res.* **2014**, *16*, 210.
[67] M. Resnicoff, E. E. Medrano, O. L. Podhajcer, A. I. Bravo, L. Bover, J. Mordoh, *Proc. Natl. Acad. Sci. U. S. A.* **1987**, *84*, 7295.
[68] T. Gudjonsson, L. Rønnov-Jessen, R. Villadsen, F. Rank, M. J. Bissell, O. W. Petersen, *J. Cell Sci.* **2002**, *115*, 39.
[69] J. Yang, R. A. Weinberg, *Dev. Cell* **2008**, *14*, 818.

